



HAL
open science

Influence of shallow traps on the enhancement of the photorefractive grating amplitude by a high-frequency alternating electric field: a probabilistic analysis

Ivan Biaggio, Gérald Roosen

► To cite this version:

Ivan Biaggio, Gérald Roosen. Influence of shallow traps on the enhancement of the photorefractive grating amplitude by a high-frequency alternating electric field: a probabilistic analysis. *Journal of the Optical Society of America B*, 1996, 13 (10), pp.2306-2314. hal-00861450

HAL Id: hal-00861450

<https://hal-iogs.archives-ouvertes.fr/hal-00861450v1>

Submitted on 12 Sep 2013

HAL is a multi-disciplinary open access archive for the deposit and dissemination of scientific research documents, whether they are published or not. The documents may come from teaching and research institutions in France or abroad, or from public or private research centers.

L'archive ouverte pluridisciplinaire **HAL**, est destinée au dépôt et à la diffusion de documents scientifiques de niveau recherche, publiés ou non, émanant des établissements d'enseignement et de recherche français ou étrangers, des laboratoires publics ou privés.

Influence of shallow traps on the enhancement of the photorefractive grating amplitude by a high-frequency alternating electric field: a probabilistic analysis

Ivan Biaggio* and Gérald Roosen

Institut d'Optique Théorique et Appliquée, Unité de Recherche Associée 14 au Centre National de la Recherche Scientifique, Bât. 503, B.P. 147, Centre Scientifique d'Orsay, F-91403 Orsay Cedex, France

Received December 18, 1995; revised manuscript received February 26, 1996

We calculate the photorefractive grating amplitude in the presence of a high-frequency applied electric field in terms of the mean-square drift length of the charge carriers. We describe how a shallow-trap level and the related long effective deep-trap recombination time are detrimental to the enhancement produced by a square-wave field. We give expressions for the shallow-trap-induced reduction in the steady-state photorefractive gain as well as for its frequency dependence. The photorefractive gain reaches the same value obtained in the one-level model at low frequencies but falls almost exponentially to a shallow-trap-limited value for higher frequencies. We compare the predictions of our model with other existing models and with experimental data. © 1996 Optical Society of America.

1. INTRODUCTION

The application of a square-wave alternating electric field during holographic recording in a photorefractive crystal leads to large grating amplitudes and a large photorefractive gain.¹ In Refs. 1 and 2 analytical expressions for the space-charge field have been derived under the main assumption that the frequency of the applied field is much smaller than the recombination rate of the photoexcited charge carriers. The frequency dependence of the space-charge field amplitude at high frequencies, where the modulation period becomes of the order of the free-carrier lifetime, was calculated in Ref. 3. In Ref. 4 the band-transport model was solved numerically in the presence of two levels, one deep and one shallow. The treatments in Refs. 3 and 4 are quite complex and involve a fair number of parameters. They are difficult to use for describing the basic processes that limit the space-charge field amplitude at high frequencies. To our knowledge, no simple analytical solution for the enhancement of the space-charge field amplitude in the presence of a shallow-trap level has been published yet.

We show that at grating spacings larger than diffusion and drift lengths it is possible to simplify the problem and to understand the limits to the enhancement mechanism by considering only the relevant time constants that describe charge-carrier excitation and recombination processes. The enhancement effect of an alternating field can be understood for all the frequencies higher than the photorefractive response rate on the basis of a simple probabilistic model. The high-frequency ac field increases the mean-square length traveled by a charge carrier between photoexcitation and recombination. We use this mean-square length to calculate the space-charge field amplitude obtained under an ac field.

This approach presents several advantages: It is valid

for all the applied-field frequencies larger than the photorefractive response rate; the resulting space-charge field can be described only in terms of the mobility–lifetime product and the characteristic time constants; and the model can be adapted to account for changing experimental realities, such as multiple levels or other field wave forms, with minimum modification.

First we briefly review the simplest case already treated in Ref. 1, then we use probability theory to calculate the influence of an applied-field period comparable with the free-carrier lifetime,³ and finally we study the case in which a shallow-trap level is present. We derive simple analytical expressions that give the amplitude of the photoinduced space-charge field as a function of the characteristic time constants that describe recombination in the two levels and the thermal excitation time from the shallow level.

2. DESCRIPTION OF THE BASIC APPROACH

A photorefractive crystal is illuminated by two interfering light beams that give rise to a low-contrast sinusoidal interference pattern. In the presence of a single trap level and an applied ac field with a time period much longer than the free-charge-carrier lifetime and much shorter than the photorefractive response time, the sinusoidal steady-state space-charge field is phase shifted by $\pi/2$ with respect to the light fringes. Its amplitude is^{1,2}

$$E_{sc} = m \frac{E_q E_{D'}}{E_q + E_{D'}}, \quad (1)$$

where m is the modulation of the light interference pat-

tern and is assumed to be small (m is given by the ratio between the amplitude of the sinusoidal intensity modulation and the average intensity).

E_q is the well-known trap-limited field

$$E_q = \frac{eN}{\epsilon\epsilon_0 K_g}, \quad (2)$$

with e being the unit charge; ϵ , the effective dielectric constant; N , the effective impurity center density; and K_g , the modulus of the grating wave vector.

$E_{D'}$ is a modified diffusion field given by

$$E_{D'} = K_g \left(\frac{k_B T}{e} + \frac{\mu \tau E^2}{1 + K_g^2 L_D^2} \right), \quad (3)$$

where k_B is Boltzmann's constant, T is the absolute temperature, μ is the mobility of the charge carriers, τ is their lifetime, E is the amplitude of the applied field, and L_D is the charge-carrier diffusion length given by $L_D^2 = \mu \tau k_B T / e$. Because the absolute value of the applied electric field is constant (it is a square-wave field), the effect of a higher, electric-field-induced charge-carrier temperature can be taken into account by use of the correct mobility value for every applied field amplitude. For simplicity, we do not introduce an explicit electric-field dependence of the mobility.

Equations (1)–(3) are obtained from the space-charge field expression given in Ref. 1 by straightforward algebra. We prefer the form of Eqs. (1)–(3) because it is easier to interpret physically. Equation (1) has the same form as in the classical photorefractive model with no applied field.⁵ The space-charge field amplitude is given by the modified diffusion field $E_{D'}$ when it is significantly smaller than the trap-limited field. It is given by the trap-limited field E_q when $E_{D'}$ is much larger than E_q . When the applied field is zero, the field $E_{D'}$ is the diffusion field $E_D = K_g k_B T / e$, and Eq. (1) develops into the classical solution. We also use Eq. (1) in connection with the results that we obtain below by our probabilistic approach.

The influence of the high-frequency applied field is concentrated in the second term on the right-hand side of Eq. (3). The alternating electric field leads to an effective diffusion field $E_{D'}$ that is larger than the normal diffusion field describing the thermal movement of the charges. At grating spacings much larger than the diffusion length, the denominator of the second term becomes negligible (its value tends to 1). The enhancement effect of the applied ac field is equivalent to a higher temperature. From Eq. (3) we can see that strong enhancements of the holographic recording efficiency can be obtained when the drift length induced by the external field becomes larger than the diffusion length [$(\mu \tau E)^2 > \mu \tau k_B T / e$]. This is the main condition for a square-wave applied field. It is not important how the drift length relates to the grating spacing.

Below we describe photoassisted charge transport by means of a random-walk model. Using this approach, we are able to describe the charge transport caused by thermal diffusion as well as the charge transport induced by the applied ac field. We define the step length of the random walk as the random distance that a charge carrier

moves before it recombines on the same impurity level as that from which it was excited. The contribution of drift to charge transport can be taken into account by the random-walk approach if each drift-dependent charge displacement has an equiprobable random direction. This is true in the case of an applied field with a period much shorter than the photorefractive response time because the photoexcitation time of every charge carrier is randomly distributed with respect to the phase of the ac field. A photoexcited charge has equal chances of finding a positive or a negative electric field.

The fundamental assumption that must be fulfilled to describe the macroscopic charge transport with a random walk is that the macroscopic charge redistribution must be produced by a large number of uncorrelated photoexcitation–recombination steps. The number of individual steps must be large in any time interval of interest. When the illumination pattern is in the form of a plane-wave grating, this amounts to neglecting diffusion length and drift length when compared with the grating spacing. Our model is thus a long grating spacing approximation. The experimental conditions under which it can be applied are very easy to realize.

Consider the basic relation between the random-walk description and diffusion. A diffusion process described by a diffusion equation

$$\frac{dn}{dt} = D \frac{d^2 n}{dx^2} \quad (4)$$

corresponds to a random movement of particles with density n , with each particle performing a random walk. The diffusion constant D is related to the efficiency of the diffusion process. In this one-dimensional example the random walk consists of steps in the $\pm x$ direction. The steps are characterized by a mean-square length $\langle L^2 \rangle$ and by an average step time τ . In any time interval Δt where $\Delta t / \tau \gg 1$ the effect of the random walk on a population of particles is given by Eq. (4), with

$$D = \frac{\langle L^2 \rangle}{2\tau}. \quad (5)$$

We describe the light-induced redistribution of charges that leads to the photorefractive effect in terms of a random walk, with each step being given by the charge displacement that takes place between photoexcitation and recombination of a charge carrier in the same level as that from which it was excited. The step time τ corresponds to the recombination time (which is the same as the free-carrier lifetime if only one trap level is present). When no electric field is applied to the sample, $\langle L^2 \rangle$ is the mean-square diffusion length $\langle L_D^2 \rangle = 2\mu \tau k_B T / e$, and D is given by the Einstein relation $D = \mu k_B T / e$.

Using our assumption that the ac field period is much shorter than the photorefractive response time, we can describe the ac field only in terms of the mean-square step length that it induces. $\langle L^2 \rangle$ also contains a term related to random drift. The diffusion constant given in Eq. (5) and the classical band conduction model⁵ can be used in the usual way to derive the steady-state space-charge field amplitude. The result has the same form as is given in Eq. (1).

We do not repeat here the complete derivation of Eq. (1) in the standard band conduction model, but we give a short derivation of the effective diffusion field as a function of $\langle L^2 \rangle$. Consider the effect of diffusion when a sinusoidal light interference pattern produces a sinusoidal modulation in the photoexcitation rate. Steady state is reached when the average charge displacement induced by diffusion is exactly compensated by the charge displacement induced by the space-charge field that is built up. At long grating spacings the grating amplitude reaches a value E_0 that is given by the equilibrium of diffusion- and space-charge-field-induced drift current:

$$D \frac{dn}{dx} = \mu n E_0. \quad (6)$$

For a sinusoidal grating $n(x) = n_0[1 + m \cos(K_g x)]$ and a small modulation index m , Eqs. (5) and (6) lead in the first order to $E_0 = m[K_g \langle L^2 \rangle / (2\tau\mu)] \sin(K_g x)$. This can be written as $E_0 = m E_D' \sin(K_g x)$, where $E_D' = K_g \langle L^2 \rangle / (2\tau\mu)$ is the effective diffusion field. When only thermal diffusion is present, E_D' does not depend on the mobility or the lifetime of the charge carriers. The steady-state grating amplitude depends on the average charge-carrier displacement produced by a single excitation-recombination step and on the average step time τ . It does not depend on the rate with which charges are displaced; i.e., it does not depend on the optical intensity.

The mean-square step length $\langle L^2 \rangle$ can be expressed as a sum of a term arising from thermal diffusion and a term arising from random drift. In the presence of an applied alternating electric field we define $\langle L_E^2 \rangle$ as the mean-square value of the distance that a charge carrier drifts between a photoexcitation and a recombination event. Because diffusion and drift are both random and uncorrelated, the mean-square value of the total random-walk step length is given by the sum of the mean squares of diffusion and drift lengths, respectively: $\langle L^2 \rangle = \langle L_D^2 \rangle + \langle L_E^2 \rangle$. The diffusion constant in Eq. (6) then contains a diffusion term and a drift term. The effective diffusion field describing thermal diffusion as well as random drift is

$$E_D' = \frac{K_g}{2\mu\tau} (\langle L_D^2 \rangle + \langle L_E^2 \rangle). \quad (7)$$

To obtain the space-charge field amplitude under an applied alternating field one must calculate $\langle L_E^2 \rangle$ and insert Eq. (7) into Eq. (1).

For a constant electric field with amplitude E and a charge carrier with a lifetime τ , $\langle L_E^2 \rangle = 2\langle |L_E| \rangle^2 = 2(\mu\tau E)^2$. This result is derived from the exponential probability density giving the distribution of charge-carrier lifetimes:

$$P(t) = \frac{1}{\tau} \exp(-t/\tau), \quad (8)$$

where τ represents the average lifetime of a free charge carrier.

Let us now calculate the value of E_D' for an alternating electric field with a time period θ much longer than the charge-carrier lifetime (this is the case that we presented

at the beginning of this section and which has been treated in Ref. 1). A charge carrier photoexcited at a time t will drift by an average length $L_E(t) = \mu\tau E(t)$, where $E(t)$ is the electric-field value at photoexcitation time. Because t can assume any value between 0 and θ in an equiprobable way, the resulting mean-square drift length is given by the average over all possible values of t :

$$\langle L_E^2 \rangle = \frac{2}{\theta} \int_0^\theta [\mu\tau E(t)]^2 dt, \quad (9)$$

The maximum value of $\langle L_E^2 \rangle$ is obtained when $E(t)$ is a perfect square wave. Because $\tau \ll \theta$, the probability that the field changes sign during the lifetime of the charge carrier is negligible in such a case, and the drift length is independent of excitation time. The resulting mean-square value is $\langle L_E^2 \rangle = 2(\mu\tau E)^2$. We insert this value into Eq. (7) to obtain

$$E_D' = K_g \left(\frac{k_B T}{e} + \mu\tau E^2 \right). \quad (10)$$

This expression is the same as the result in Eq. (3), but without the factor $(1 + K_g^2 L_D^2)$ in the denominator of the second term. This is because our approach is a long grating spacing approximation. In Eq. (3) the $(1 + K_g^2 L_D^2)$ denominator diminishes the effect of the applied field at grating spacings shorter than the diffusion length. It reduces the importance of an enhancement of the step length between photoexcitation and recombination when its thermally induced value is already larger than the grating period.

It is possible to rewrite Eq. (3) as a function of the mean-square drift length $\langle L_E^2 \rangle$:

$$E_D' = K_g \left[\frac{k_B T}{e} + \frac{\langle L_E^2 \rangle}{2\tau\mu(1 + K_g^2 L_D^2)} \right]. \quad (11)$$

This expression, like Eq. (7), gives the effective diffusion field as a function of the mean-square thermal diffusion length, the mean-square drift length, and the mobility-lifetime product. It assumes that the applied electric field is a square wave.

Below we calculate the mean-square drift length $\langle L_E^2 \rangle$ for an applied square-wave field in the general cases in which the lifetime of the charge carriers is comparable with the electric-field period and when a second, shallow-trap level is present. We show that a change in the applied-field period changes only $\langle L_E^2 \rangle$. Because of this fact it is possible to use Eq. (11) instead of Eq. (7) to calculate the resulting space-charge field. When the long grating spacing approximation is fulfilled, Eq. (11) and Eq. (7) give the same result. When the diffusion length is not completely negligible with respect to the grating spacing, Eq. (11) ensures that the space-charge field amplitude becomes exactly the value given by Eqs. (1)–(3) in the limit in which the assumptions of Ref. 1 are fulfilled (i.e., only one trap level and a recombination time τ much smaller than the electric-field period θ). Note, however, that Eq. (11) is only an *ad hoc* expression valid in the case in which the applied field is a square wave, whereas Eq. (7) is always valid at long grating spacings.

In the short-lifetime approximation that we used above, where $\tau \ll \theta$, it is very easy to calculate from Eq.

(9) the mean-square drift length corresponding to any wave form of the applied field. Deviation from a perfect square wave leads to a diminished photorefractive gain because the probability that a photoexcited charge carrier finds an electric field value near zero becomes appreciable. In a sinusoidal ac field, Eq. (9) delivers a mean-square drift length that is a factor of 2 smaller than that found in the optimal square-wave case. This corresponds to the long grating spacing limit of the space-charge field expression for a sinusoidal ac applied field given in Ref. 1.

3. CHARGE-CARRIER LIFETIME COMPARABLE WITH THE APPLIED-FIELD PERIOD

When the average charge-carrier lifetime is comparable with the applied-field period, one has to calculate the mean-square value of the step length while taking into account the probability that the field switches its sign during the life of the charge carrier.

If a charge carrier lives a time longer than a full period θ of the applied field, the drifts obtained during the positive and the negative half-periods will compensate each other. To calculate the expectation value of the drift length, one can fold all the equivalent lifetimes that differ by multiples of θ to the time interval from zero to θ and can define an effective folded time t . The corresponding probability density P_f is

$$\begin{aligned} P_f(t) &= \sum_{n=0}^{\infty} \frac{1}{\tau} \exp\left(-\frac{n\theta + t}{\tau}\right) \\ &= \frac{1}{\tau} \exp(-t/\tau) \frac{1}{1 - \exp(-\theta/\tau)}, \end{aligned} \quad (12)$$

where $0 < t < \theta$. The expectation value for the squared step length L_E^2 is given by

$$\langle L_E^2 \rangle = \int_0^{\theta} L^2(t) P_f(t) dt, \quad (13)$$

where $L^2(t)$ must be calculated with consideration of the square-wave electric field and the fact that its phase can assume any value between 0 and 2π in an equiprobable way. We calculate $\langle L_E^2 \rangle$ in two steps: by first integrating over all possible excitation times, and then integrating over all possible lifetimes, using Eq. (13).

As an example, we calculate $L^2(t)$ when $t < \theta/2$. The probability $P^{+/-}$ that a time segment of length t intersects one of the two electric-field switch times found in the time segment of length θ is $P^{+/-} = (2t)/\theta$. When this event occurs, the charge carrier drifts in one direction during a time $(t - t_s)$ and in the opposite direction during a time t_s , where t_s denotes the moment when the electric-field switches sign. t_s is randomly distributed in an equiprobable way between 0 and t . The average of the square drift length over all possible excitation times is thus in this case

$$L_{+/-}^2(t) = \frac{(\mu E t)^2}{t} \int_0^t [(t - t_s) - t_s]^2 dt_s = \frac{(\mu E t)^2}{3}. \quad (14)$$

The probability that a time segment of length t does not intersect the time when the electric-field switches sign is $P^{+/-} = (1 - P^{+/-})$, and in such a case the average of the square drift length is simply $L_{+/-}^2(t) = (\mu E t)^2$. The total average value of the squared step length is given by $P^{+/-} L_{+/-}^2 + (1 - P^{+/-}) L_{+/-}^2$. The result is

$$L^2(t)|_{t < \theta/2} = (\mu E t)^2 \left(1 - \frac{4t}{3\theta}\right). \quad (15)$$

In the same way, we can calculate the excitation-time average of the squared step length when $t > \theta/2$. The result has the same form as Eq. (15), but with $(\theta - t)$ being substituted for t . Inserting these values of the squared step length into Eq. (13) and changing integration variables, we obtain

$$\langle L_E^2 \rangle = \mu^2 E^2 \int_0^{\theta/2} t^2 \left(1 - \frac{4t}{3\theta}\right) [P_f(t) + P_f(\theta - t)] dt, \quad (16)$$

which is equal to

$$\langle L_E^2 \rangle = 2(\mu E \tau)^2 \left[1 - \frac{4\tau}{\theta} \frac{1 - \exp(-\theta/2\tau)}{1 + \exp(-\theta/2\tau)}\right]. \quad (17)$$

We obtain the space-charge field amplitude as a function of the applied-field frequency by inserting Eq. (17) into Eq. (11) and using Eq. (11) with Eqs. (1) and (2). The mean-square drift length in Eq. (17) equals $2(\mu E \tau)^2$ for a long applied-field period θ and decreases to zero when θ becomes shorter than the free-charge-carrier lifetime. This happens because the largest possible value of the drift length is always given by $\mu E \theta/2$. When the field period tends to zero, $\langle L_E^2 \rangle$ must tend to zero: The space-charge field amplitude goes back to the value obtained without any applied field.

The above solution was compared with the expression presented in Ref. 3, and we confirmed the exact correspondence of the results in the limit in which the diffusion length and the drift length are much smaller than the grating spacing.

4. INFLUENCE OF SHALLOW TRAPS

The above treatment describes the detrimental effect of a free-charge-carrier lifetime becoming comparable with the period of the applied alternating electric field. This effect is rarely a problem in practice because in most materials and at commonly used light intensities the lifetime remains much smaller than the photorefractive response time so that a wide bandwidth is available for the frequency of the applied field.

However, sizeable concentrations of shallow traps are not unusual in photorefractive materials. A shallow-trap level is only a few fractions of an electron volt away from the conduction- or valence-band edge, and charge carriers that are trapped in it are reemitted by thermal excitation. Such a shallow-trap level increases the time that it takes for a photoexcited charge carrier to return to the deep-trap level and can have important effects on the space-charge field amplitude obtained under an applied ac electric field.

We consider a shallow-trap level described by a trapping time constant τ_2 and a thermal excitation time τ_{th} , and a deep level with a trapping time constant τ_1 , as depicted schematically in Fig. 1. These three time constants are enough to describe the two levels. Thermal emission from the deep level corresponds to a low-intensity homogeneous illumination, and we do not explicitly take it into account. For simplicity, we assume that photoexcitation from the shallow-trap level is negligible compared with thermal excitation and that the photorefractive grating comes principally from charge redistribution in the deep level. We further assume that the characteristic times describing the two levels are constants (i.e., we assume little shallow-trap filling, or constant homogeneous filling at a constant light intensity). The model can be applied to electron transport as well as hole transport.

We first discuss the influence of shallow traps on the main parameters of our problem. Some of these results have been discussed in Refs. 6–8, mostly in the limit where $\tau_2 \ll \tau_1$. Here we state a few useful relationships without making any assumptions on the relative magnitudes of τ_1 , τ_2 , and τ_{th} .

For the two-level system shown in Fig. 1, the average lifetime of a photoexcited charge carrier is given by

$$\tau_0^{-1} = \tau_1^{-1} + \tau_2^{-1}. \quad (18)$$

After photoexcitation or thermal excitation a charge carrier will live an average time τ_0 and will then recombine in either one of the two levels. The probability that the charge carrier ends up in the shallow-trap level is

$$p_2 = \tau_1 / (\tau_1 + \tau_2) \quad (19)$$

and is τ_1/τ_2 times larger than the probability of recombining in the deep level. When p_2 is appreciable, the charge carrier will be trapped in the shallow-trap level and will go through a number of thermal excitation and trapping cycles before recombining into the deep level. The average span of time τ_{deep} between photoexcitation and recombination into the deep level can be found by use of a weighted sum over all possible paths leading to final recombination in a deep trap: $\tau_{deep} = \tau_0 + p_2[(\tau_{th} + \tau_0 + p_2(\tau_{th} + \tau_0 + \dots))]$. This series is easily summed to yield

$$\tau_{deep} = \tau_1(1 + \tau_{th}/\tau_2). \quad (20)$$

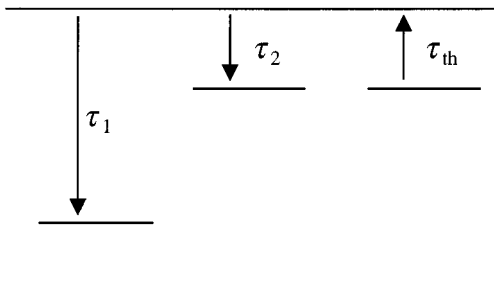


Fig. 1. Definition of the relevant time constants. τ_1 is the time constant that describes trapping into the deep level, τ_2 is the time constant that describes trapping into the shallow level, and τ_{th} is the thermal excitation time from shallow traps.

The total average time spent as a free charge carrier in the conduction or the valence band between photoexcitation and final recombination into the deep trap is always τ_1 , independent of shallow-trap concentration. The total average time spent by a charge carrier in shallow traps, waiting for thermal excitation, is given by $\tau_{th}\tau_1/\tau_2$. From the point of view of charge redistribution in the deep level, it is as though the charge carrier had a longer effective lifetime, given by Eq. (20), and a smaller effective mobility. This trap-limited mobility is

$$\mu_t = \mu(1 + \tau_{th}/\tau_2)^{-1}. \quad (21)$$

Multiplying Eq. (20) by Eq. (21), one can see that the product of trap-limited mobility μ_t and effective deep-trap recombination time τ_{deep} is always given by the band mobility multiplied by τ_1 and is independent from shallow-trap concentration.⁷ Charge redistribution within the deep level can be described by effective drift and diffusion lengths, defined as distances traveled by a charge carrier between photoexcitation and recombination into the deep traps. The effective drift and diffusion lengths are not influenced by the shallow-trap level.

The larger effective deep-trap recombination time [Eq. (20)] induced by a shallow-trap level can easily be of the order of seconds. A shallow-trap level limits the effectiveness of a square-wave applied field whenever the field period becomes shorter than the effective deep-trap recombination time τ_{deep} . Below we describe this effect using the same probabilistic approach that we used above for the one-level case. In contrast to a numerical simulation of the full band conduction model such as that of Ref. 4, this description concentrates on the most important material parameters and makes it possible to identify the main physical mechanisms that limit the effectiveness of a square-wave applied field.

In the presence of shallow traps the characteristic steplength of the random walk is the distance traveled by the charge carrier from its photoexcitation out of the deep level until its recombination into the deep level. Between these two events the carrier can be captured in the shallow-trap level and can be thermally excited any number of times. The characteristic step time is $\tau_{deep} = \tau_1(1 + \tau_{th}/\tau_2)$ [Eq. (20)]. The trapping times as well as the thermal excitation times obey the usual exponential probability distributions.

Although all the probabilities are simple and well defined, calculation of the mean-square step length $\langle L_E^2 \rangle$ from probability theory appears to be cumbersome in the general case in which the applied-field period is comparable with the step time. It is, however, very easy to obtain the correct solution from a simple Monte Carlo simulation: One generates a random free-carrier lifetime and random excitation times according to their probability distributions and then uses them and the given applied-field period to calculate L_E^2 . This process is repeated a large number of times. The expectation value $\langle L_E^2 \rangle$ is equal to the average over all the random L_E^2 values.

The single steps of the Monte Carlo calculation are

- (0) Create a charge carrier at a random time t_{ex} .
- (1) Generate a random free-carrier lifetime Δt according to its exponential probability density [Eq. (8)]. Given a random number r homogeneously distributed between 0

and 1, Δt is obtained from $\Delta t = -\tau_0 \ln(r)$, where τ_0 is the average free-carrier lifetime given by Eq. (18).

(2) Calculate the drift length L_i from t_{ex} and Δt , taking into account the phase and the periodicity of the applied field.

(3) Decide if trapping took place in the shallow-trap level. One does this by generating a random number r between 0 and 1 and checking whether $r < p_2 = (1 + \tau_2/\tau_1)^{-1}$ [Eq. (19)].

(4) If the test in point (3) is passed, generate a random thermal excitation time and go back to point (1). If the test in point (3) is not passed (recombination takes place in the deep level), calculate $L_E^2 = (\sum L_i)^2$.

(5) Store the L_E^2 calculated in point (4), and go back to point (0).

After points (0)–(5) have been iterated a sufficient number of times, the average $\langle L_E^2 \rangle$ over all the simulated L_E^2 values can be calculated. One obtains the space-charge field amplitude as before, by inserting $\langle L_E^2 \rangle$ into Eq. (11) and using the result in Eq. (1). The numerical implementation of points (0)–(5) in a high-level programming language is less than 50 lines long and can run efficiently on a desktop computer.

Figure 2 gives the frequency dependence of the space-charge field amplitude obtained in this way. The curves were calculated with 10,000 iterations and with a parameter set as close as possible to the one used by Moisan *et al.*⁴ for their Fig. 15. The time constants were derived from the trap concentrations and from the capture and the excitation cross sections given in Ref. 4 and are $\tau_1 = 1.25$ ns, $\tau_2 = 0.022$ –2.2 ns, $\tau_{th} = 50$ μ s. We used a hole mobility of 80 cm²/(V s).

The drift length obtained with the above parameters is already comparable with the grating spacing, so we are no longer in the region in which the probabilistic model is

strictly valid. Moreover, the numerical simulation of Ref. 4 considers a large number of material parameters, whereas our approach describes the two levels with only three parameters. In spite of this, the two models agree well when one is describing the frequency dependence above 50 Hz, i.e., for applied-field frequencies larger than the photorefractive response rate (see Fig. 2 and Ref. 4, Fig. 15; the numerical calculation of Ref. 4 includes the effects of the photorefractive response time and is also valid at low frequencies).

Figure 2 shows that the shallow-trap level does not have any influence at low applied-field frequencies. The reason is that in this case the effective deep-trap recombination time $\tau_{deep} = \tau_1(1 + \tau_{th}/\tau_2)$ is still much shorter than the period of the ac field, and $\langle L_E^2 \rangle$ is given by $2(\mu\tau_1 E)^2 = 2(\mu\tau_{deep} E)^2$. This is the same result as for a single level.

In the interesting case in which the applied-field period θ remains longer than the free-charge-carrier lifetime τ_0 , one can calculate analytically the space-charge field amplitude in both the low- and the high-frequency regions of Fig. 2. This gives an expression for the amount of the shallow-trap-induced reduction in space-charge field amplitude that is observed at higher applied-field frequencies.

This reduction is directly correlated to the decreased efficiency of the random drift process when the period of the applied field becomes shorter than the effective deep-trap recombination time τ_{deep} . At applied-field periods θ much smaller than both the τ_{deep} value and the thermal reexcitation time τ_{th} , the correlation between the drift direction after every thermal excitation that existed for $\theta \gg \tau_{deep}$ is lost. Each thermal reexcitation is now a random event leading to an independent step length, and one must add the mean squares of the step lengths occurring

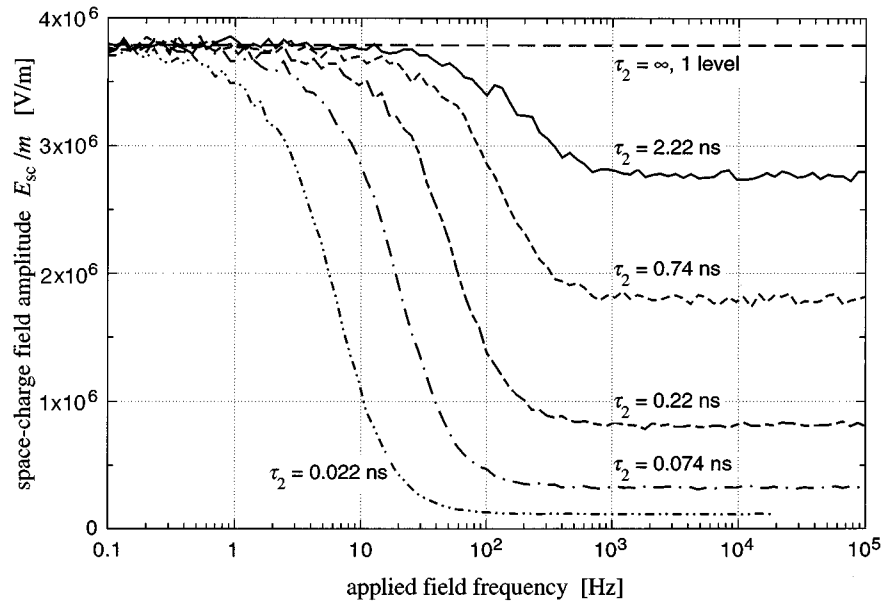


Fig. 2. Calculated space-charge field amplitude E_{sc}/m as a function of the applied-field frequency in the presence of shallow traps. Monte Carlo simulation with the following parameters: $\tau_1 = 1.25$ ns, $\tau_{th} = 0.5$ ms, effective trap density $N = 4 \times 10^{16}$ cm³, effective dielectric constant $\epsilon = 10.3$, grating spacing $\Lambda_g = 10$ μ m, applied-field amplitude $E = 10$ kV/cm. The horizontal dashed line corresponds to the one-level case, whereas the other curves indicate the behavior in the presence of a shallow-trap level with a characteristic trapping time τ_2 from 2.22 to 0.022 ns.

after thermal excitation. The mean-square step length obtained for each photoexcitation event is thus

$$\begin{aligned} \langle L_E^2 \rangle &= 2(\mu\tau_0 E)^2 + p_2\{2(\mu\tau_0 E)^2 \\ &\quad + p_2[2(\mu\tau_0 E)^2 + \dots]\} \\ &= 2(\mu\tau_0 E)^2 \frac{1}{1 - p_2}, \end{aligned} \quad (22)$$

where we recall that τ_0 is the average free-carrier lifetime [Eq. (18)] and $p_2 = \tau_1/(\tau_1 + \tau_2)$ is the probability that a charge carrier recombines into the shallow-trap level rather than into the deep level [Eq. (19)]. Equation (22) can be rewritten as

$$\langle L_E^2 \rangle = \frac{2(\mu\tau_1 E)^2}{1 + \tau_1/\tau_2} = \frac{\langle L_E^2 \rangle_{\text{one level}}}{1 + \tau_1/\tau_2}. \quad (23)$$

Because one obtains the electric-field enhancement [Eq. (11)] from $\langle L_E^2 \rangle$ by dividing it by the mobility-lifetime product, which is the same for a single level or in the presence of shallow traps, Eq. (23) can be used to calculate the difference between the two frequency-independent plateaus in the frequency dependence of the space-charge field amplitude (see Fig. 2). At long grating spacings, the space-charge field amplitude can be much smaller than the limit given by the trap-limited field E_q , whereas at the same time the applied-field amplitude can be so high that thermal diffusion is negligible. In such a case the space-charge field amplitude depends linearly on $\langle L_E^2 \rangle$, and the ratio between the space-charge field amplitudes corresponding to the low- and the high-frequency plateaus in Fig. 2 is approximately given by the factor $(1 + \tau_1/\tau_2)$ in Eq. (23). The space-charge field amplitude makes a transition from its low-frequency value to a value $1 + \tau_1/\tau_2$ times smaller when the half-period of the applied field is of the order of the effective deep-trap recombination time $\tau_{\text{deep}} = \tau_1(1 + \tau_{\text{th}}/\tau_2)$ [Eq. (20)]. In Fig. 2, τ_{deep} ranges from 28 to 0.28 ms.

Note that Fig. 2 uses a logarithmic frequency axis. The curves plotted in this figure are very similar to exponential decays. [An exponential decay $\exp(-x)$ on a logarithmic x axis is represented by a curve that is horizontal at low values of x and makes a transition to zero in approximately one decade, with the exponential time constant corresponding to the inflection point of the curve.] The space-charge field amplitude shown in Fig. 2 decays more or less exponentially, with a decay time constant given by τ_{deep} , to the constant value obtained in Eq. (23). When $\tau_2 < \tau_1$ the decays from the one-level space-charge field amplitude to the shallow-trap-limited space-charge field amplitude can be closely approximated by the one-level solution of Eq. (17), with τ_{deep} being substituted for τ .

5. INTENSITY DEPENDENCE

Illumination of the crystal will cause a charge redistribution between the deep level and the shallow level. Under illumination the shallow traps will tend to fill, especially if the thermal excitation time τ_{th} is relatively long. The time constants τ_1 and τ_2 used in the above expressions for

the shallow-trap model are inversely proportional to the concentration of empty deep traps and empty shallow traps, respectively, and will therefore be intensity dependent.

The intensity dependence of these characteristic times must be considered when one is comparing experimental results with the analytical solutions given above. One can easily obtain τ_1 and τ_2 as a function of intensity by solving the equations describing excitation and recombination in each level in the steady state, under the assumption that the contrast in the illumination pattern is low (so that the zeroth-order solutions for homogeneous illumination can be used). Here we give only an expression related to the intensity dependence of the shallow-trapping time constant τ_2 . Derivation of complete expressions for the intensity dependence of τ_1 and τ_2 from the equilibrium equations in the steady state is trivial if all the material parameters are known.

Using our earlier assumption that the thermal excitation time from shallow traps is much smaller than the photoexcitation time, we find that the shallow-trapping time constant τ_2 obeys the relation

$$\tau_2(I) = \tau_2(I = 0) + \frac{\tau_{\text{th}}}{N_{\text{st}}} n(I), \quad (24)$$

where N_{st} is the total density of shallow traps and $n(I)$ is the density of free charge carriers under an illumination intensity I . We can see that τ_2 starts from its minimum value at small intensities and then grows linearly with the conductivity of the crystal, which means that it will increase when the long grating spacing photorefractive response time decreases.⁵ The effect is seen to be strong when the thermal reexcitation time from shallow traps is long or when the total density of shallow traps is low.

Although τ_2 increases with intensity, τ_1 can only decrease with intensity: Empty deep traps are created as charges are transferred from the deep level to the shallow level. We thus expect the ratio τ_2/τ_1 to become larger at larger intensities. This will increase the frequency at which the space-charge field amplitude drops to the shallow-trap-limited value [Eq. (20)]. The magnitude of the reduction will decrease [Eq. (23)].

6. DISCUSSION

The probabilistic approach demonstrates that there is a direct connection between the shallow-trap-induced larger effective deep-trap recombination time and the frequency dependence of the photorefractive grating amplitude. In materials in which shallow traps are present, we thus expect the two-wave mixing photorefractive gain to depend on the applied-field frequency in a peculiar manner. Consider the situation in which the effective deep-trap recombination time τ_{deep} induced by the shallow-trap level is appreciably smaller than the photorefractive response time. In this case the gain first increases with frequency according to the discussion in Ref. 2. The gain then saturates at the magnitude predicted by the one-level theory for applied-field periods smaller than the photorefractive response time.^{1,2} At still higher frequencies the detrimental influence of shallow traps appears. The gain follows the behavior depicted in Fig.

2: When the applied-field period becomes smaller than the effective deep-trap recombination time [Eq. (20)], the gain falls to the shallow-trap-limited value [Eq. (23)]. The electric-field enhancement will then disappear at much higher frequencies, when the applied-field period becomes comparable with the free-charge-carrier lifetime.³

A similar frequency dependence has in fact been observed in CdTe crystals in Refs. 4 and 9 and in Bi₁₂SiO₂₀ crystals in Refs. 10 and 11. In these experiments the photorefractive gain typically peaks at an optimal frequency only slightly larger than the photorefractive response rate and then falls to a smaller high-frequency value.

In Ref. 4 a numerical solution of the band-transport level in the presence of shallow traps could reproduce the observed behavior with a given set of material parameters, and the frequency dependence was attributed to the influence of shallow traps. In Ref. 12 the explanation given for a similar frequency dependence in Bi₁₂SiO₂₀ was the emergence of spatial subharmonics.

In the following the experimental results reported in Refs. 4 and 9–11 are compared with the predictions of the general treatment that we presented above, and the properties that a shallow-trap level must have to explain all the experimental data are discussed semiquantitatively.

In the data sets presented in Refs. 4, 9, and 10, the gain never manages to reach the true one-level value before it is depleted by the influence of shallow traps. The photorefractive gain goes through a low-frequency peak that is generally less than a frequency decade wide. This would be the case if the cutoff frequency given by the photorefractive response time² were only slightly smaller than the inverse of the effective deep-trap recombination time [Eq. (20)]. The maximum value of the photorefractive gain as a function of frequency then depends on the difference between the photorefractive response time and the effective deep-trap recombination time τ_{deep} , as well as on the reduction factor in Eq. (23). Because these three factors depend on intensity, a side effect of this is that the low-frequency peak is influenced by optical intensity and other parameters determining the speed of the crystal, such as the grating spacing and the amplitude of the applied field.

For example, in all the experimental studies^{4,9,10} the same characteristic dependence on the applied-field amplitude was observed. The relative height of the photorefractive gain peak at low frequency decreases as the applied-field amplitude decreases, and the position of the peak moves slightly to higher frequencies. This happens because the photorefractive response of the crystal is faster at lower applied-field amplitudes, leading to a higher cutoff frequency for the onset of the gain enhancement. This cutoff frequency approaches the frequency at which the shallow-trap-induced decrease of the gain takes place. At the lowest applied-field amplitudes the cutoff frequency is so high that the photorefractive gain reaches its shallow-trap-limited value directly, without passing through a higher value approaching the one-level result.

When the optical intensity is increased, the photorefractive response time becomes smaller, but the shallow-trap-induced effective deep-trap recombination time [Eq.

(20)] also decreases because of the photoconductivity dependence given in Eq. (24). This can explain the fact that the gain-versus-frequency curve tends to be simply translated horizontally on a logarithmic frequency axis when the intensity is changed, as observed in Refs. 4 and 10.

The dependence of the gain-versus-frequency curve on the light wavelength is also interesting. In Ref. 9 the high-frequency decrease in gain observed in vanadium-doped CdTe is relatively strong at a laser wavelength of 1.55 μm . But at 1.06 μm the transition to a possible shallow-trap-limited value takes place at a higher frequency and is less accentuated. This is consistent with a larger τ_2 value at 1.06 μm [Eqs. (20) and (23)], which can be related to a smaller shallow-trap concentration. Because the majority charge carriers were holes at 1.55 μm and electrons at 1.06 μm , it is possible that the sample has a larger concentration of shallow hole traps and a low concentration of shallow electron traps. A hole shallow-trap level could be connected with charge compensation of the ionized deep level centers that come from the vanadium doping and could have a concentration as large as the density of ionized deep centers. Shallow electron traps are not needed for charge compensation. A low density of shallow electron traps is also consistent with the results obtained in Ref. 13, in which strong photorefractive gains at the 1.06- μm wavelength were observed in CdTe crystals at applied-field frequencies as high as 1 kHz.

The fact that the data of Refs. 4, 9, and 10 do not show a clear frequency-independent low-frequency plateau as in Fig. 2 makes it difficult to analyze the experimental results quantitatively. The different magnitudes of the peak photorefractive gain and its higher-frequency value set only a lower limit to the factor $(1 + \tau_1/\tau_2)$ used in Eq. (23). In the sample of Ref. 9 the photorefractive gain drops by approximately a factor of 3 after the low-frequency peak, which tells us that $(1 + \tau_1/\tau_2) > 3$. τ_2 is certainly smaller than τ_1 in that sample, but τ_1/τ_2 is probably not larger than 10 because the gain does not fall completely to the zero-applied-field value. Because the transition frequency is proportional to $(\tau_2/\tau_1)/\tau_{\text{th}}$ when $\tau_{\text{th}} \gg \tau_2$ [Eq. (20)], the thermal excitation time from shallow traps should be of the order of 1 ms in this sample. All the data presented in Refs. 4, 9, and 10 could be explained with a shallow-trapping time constant τ_2 that is of the same order of magnitude as the trapping time constant for deep traps τ_1 , and with thermal excitation times of the order of 1–10 ms. A separate measurement of the mobility–lifetime product or of the free-carrier lifetime τ_0 would provide extra information about τ_1 and τ_2 , thus allowing a more precise estimation of the shallow-trap parameters τ_2 and τ_{th} .

With the exception of an apparent high-frequency increase in photorefractive gain that was reported in Ref. 11, all the data in Refs. 4 and 9–11 can be qualitatively explained by our shallow-trap model, and the features in the frequency response of the photorefractive gain can be related to Eqs. (20) and (23). There are strong indications that a shallow-trap level is responsible for the observed frequency dependence of the gain. However, the available data are not complete enough to enable us to de-

cide whether all the effects are caused by a shallow-trap level or whether in some cases spatial subharmonics^{11,12} also play a role.

It is possible to design experiments in which the frequency dependence of the gain is measured at long grating spacings, so that Eqs. (1)–(3), (11), and (23) can be used to determine the shallow-trap parameters more accurately. To be able to distinguish the two plateaus in the gain-versus-frequency curve and to analyze the influence of the shallow-trap level quantitatively, one needs a photorefractive response time that is at least 10 times longer than the shallow-trap-induced effective deep-trap recombination time τ_{deep} , and the latter must clearly be longer than the applied-field period for which the slew rate of the high-voltage amplifier starts limiting the gain.¹² The frequency dependence should be measured over at least three decades centered around the transition frequency at which the photorefractive gain changes from its low-frequency value to the shallow-trap-limited value. One can increase this frequency by increasing the temperature of the sample, because τ_{th} is expected to depend exponentially on temperature.⁸

7. CONCLUSIONS

We discussed the enhancement of a photorefractive grating by an alternating applied electric field, using probability theory instead of differential equations. The treatment applies at grating spacings longer than diffusion length and drift length. In this limit we expressed the influence of shallow traps and of a long effective deep-trap recombination time as a function of only three parameters: the thermal excitation time from shallow traps, and the recombination probabilities in shallow traps and in the deep level. We provided simple analytical expressions describing the influence of the charge-carrier lifetime and of a shallow-trap level on the enhancement effect of an applied square-wave electric field.

Experiments performed at long grating spacings, where our approach is valid, can be used as a tool for material characterization. Beam coupling measurements under an applied square-wave electric field would give information on whether high concentrations of shallow traps are present in a given crystal, on the ratio between recombination probability in shallow traps and that in the deep traps, and on the thermal excitation time from shallow traps.

*Present address: Nonlinear Optics Laboratory, Institute of Quantum Electronics, Swiss Federal Institute of Technology, ETH-Hönggerberg, CH-8093 Zürich, Switzerland. E-mail address: biaggio@iqe.phys.ethz.ch.

REFERENCES

1. S. I. Stepanov and M. P. Petrov, "Efficient unstationary holographic recording in photorefractive crystals under an external alternating electric field," *Opt. Commun.* **53**, 292–295 (1985).
2. C. Besson, J. M. C. Jonathan, A. Villing, G. Pauliat, and G. Roosen, "Influence of alternating field frequency on enhanced photorefractive gain in two-beam coupling," *Opt. Lett.* **14**, 1359–1361 (1989).
3. F. Vachss, "Frequency-dependent photorefractive response in the presence of applied ac electric fields," *J. Opt. Soc. Am. B* **11**, 1045–1058 (1994).
4. J.-Y. Moisan, N. Wolffer, O. Moine, P. Gravey, G. Martel, A. Aoudia, R. Repka, Y. Marfaing, and R. Triboulet, "Characterization of photorefractive CdTe:V high two-wave mixing gain with an optimum low-frequency periodic external electric field," *J. Opt. Soc. Am. B* **11**, 1655–1667 (1994).
5. G. Valley and M. B. Klein, "Optimal properties of photorefractive materials for optical data processing," *Opt. Eng.* **22**, 704–711 (1983).
6. F. Strohkendl, "Light-induced dark decays of photorefractive gratings and their observation in Bi₁₂SiO₂₀," *J. Appl. Phys.* **65**, 3773–3780 (1989).
7. G. Pauliat and G. Roosen, "Photorefractive effect generated in sillenite crystals by picosecond pulses and comparison with the quasi-continuous regime," *J. Opt. Soc. Am. B* **7**, 2259–2267 (1990).
8. P. Nouchi, J. P. Partanen, and R. W. Hellwarth, "Simple transient solutions for photoconduction and the space-charge field in a photorefractive material with shallow traps," *Phys. Rev. B* **47**, 15581–15587 (1993).
9. Y. Belaud, P. Delaye, J.-C. Launay, and G. Roosen, "Photorefractive response of CdTe:V under ac electric field from 1 to 1.5 μm ," *Opt. Commun.* **105**, 204–208 (1994).
10. K. Magde and G. Brost, "Influence of the ac field frequency on the photorefractive response in Bi₁₂SiO₂₀," *Opt. Mater.* **4**, 322–325 (1995).
11. G. Brost, K. Magde, J. Larking, and M. Harris, "Investigation of the frequency-dependent photorefractive response with alternating electric fields in BSO," in *Digest of Topical Meeting on Photorefractive Materials, Effects, and Devices* (Optical Society of America, Washington, DC., 1995), paper MPB2, pp. 144–157.
12. A. Grunnet-Jepsen, L. Solymar, and C. H. Kwak, "Effect of subharmonics on two-wave gain in Bi₁₂SiO₂₀ under alternating electric fields," *Opt. Lett.* **19**, 1299–1301 (1994).
13. M. Ziari, W. H. Steier, P. M. Ranon, M. B. Klein, and S. Trivedi, "Enhancement of the photorefractive gain at 1.3–1.5 μm in CdTe using alternating electric fields," *J. Opt. Soc. Am. B* **9**, 1461–1466 (1992).